Bull. Mater. Sci., Vol. 40, No. 4, August 2017, pp. 691–698
DOI 10.1007/s12034-017-1412-2

Ex situ synthesis of G/α-Fe_2O_3 nanocomposite and its catalytic effect on the thermal decomposition of ammonium perchlorate

MERIEM AMINA FERTASSI[1], QI LIU[1,*], RUNZE LI[2], PINGAN LIU[2], JINGYUAN LIU[1], RONG-RONG CHEN[3], LIANHE LIU[3] and JUN WANG[1,3]

[1]Key Laboratory of Superlight Material and Surface Technology, Ministry of Education, Harbin Engineering University, Harbin 150001, People's Republic of China

[2]Metal Fuel Research Institute, College of Aerospace and Civil Engineering, Harbin Engineering University, Harbin 150001, People's Republic of China

[3]Institute of Advanced Marine Materials, Harbin Engineering University, Harbin 150001, People's Republic of China

*Author for correspondence (qiliu@hrbeu.edu.cn)

MS received 21 May 2016; accepted 26 August 2016; published online 25 July 2017

Abstract. α-Fe_2O_3 nanoparticles were prepared by a facile hydrothermal method using ferric chloride hexahydrate ($FeCl_3 \cdot 6H_2O$) as a precursor. Graphene oxide (GO) was synthesized using a modified Hummers method and graphene nanosheets (G) were successfully obtained by thermal reduction of GO. G/α-Fe_2O_3 nanocomposite was prepared using *ex situ* synthesis in the presence of α-Fe_2O_3 nanoparticles and GO solution. The characterization of the as-prepared materials was performed using X-ray diffraction analyses and Fourier transform infrared spectroscopy; their morphology was investigated by scanning electron microscopy and transmission electron microscopy; the specific surface area (S_{BET}) was determined by nitrogen adsorption; their catalytic activity on the thermal decomposition of ammonium perchlorate (AP) was investigated by differential thermal analysis (DTA). The results of DTA indicated that the obtained nanomaterials contribute in ameliorating the thermal decomposition of AP; specifically, the high decomposition temperature of AP decreases from 432 to 380°C. A significant decrease in the activation energy was also achieved in the presence of these nanomaterials, and the mixture of ammonium perchlorate with G/α-Fe_2O_3 showed the lowest value (from 129 to 80.33 kJ mol^{-1}).

Keywords. α-Fe_2O_3; graphene/α-Fe_2O_3 nanocomposite; ammonium perchlorate; thermal decomposition; catalytic activity.

1. Introduction

In nature, iron oxide exists in three types: magnetite (Fe_3O_4), maghemite (γ-Fe_2O_3) and hematite (α-Fe_2O_3). The latter is the oldest known type of iron oxide; it was used in many applications, especially as a catalyst, due to its abundance, low cost, non-toxicity and high stability. Many methods have been used before to prepare hematite (α-Fe_2O_3) nanoparticles; one of the most used methods is the hydrothermal synthesis because of its easy manipulation, scalable production and precise control of size [1].

Graphene (G) is one of the newest materials that made a great noise in different fields; this material is one of the allotropic forms of carbon with a two-dimensional structure and unique properties such as large surface area, superelectronic conductivity and excellent mechanical properties [2]. It can be obtained using different methods and the easiest one is the thermal reduction of exfoliated graphene oxide (GO) [3,4].

Ammonium perchlorate (AP) is a white crystalline substance with a specific gravity of 1.88 g cm^{-3}; it is the most used oxidant that constitutes more than 65% of composite propellants formulation [5]. Many studies show that the ballistics properties and the performance of composite propellants depend strongly on the characteristics of thermal decomposition of their oxidizers [6–8].

The thermal decomposition of AP is powerfully sensitive to additives, and particularly nanoadditives because of their small size and high surface area [9,10]. A lot of studies show that transition metal oxides nanoparticles can decrease the decomposition temperature of AP and therefore improve the ballistic properties of composite propellants [11–14]. However, due to the small size of these nanoadditives, they are likely to aggregate and expose fewer active sites. For this reason graphene/α-Fe_2O_3 nanocomposite is used here as a new additive in order to decrease the aggregation of α-Fe_2O_3 nanoparticles and improve their catalytic activity on the thermal decomposition of AP.

The present work gives a strong reason for the application of G/α-Fe_2O_3 nanocomposite in the AP-based propellant as a catalyst to improve the thermal decomposition of AP and therefore improve the ballistic properties of the composite propellant. In this paper we report on a facile synthesis of

graphene, α-Fe_2O_3 nanoparticles and G/α-Fe_2O_3 nanocomposite by a simple hydrothermal method, and their catalytic activity on the thermal decomposition of AP is investigated by TG– differential thermal analysis (DTA) analyses.

2. Experimental

2.1 *Materials*

Graphite powder was obtained from Qingdao Furunda Graphite Co., Ltd. H_2SO_4 was purchased from Luoyang Chemical Reagents Limited Company. $KMnO_4$ was obtained from a Heilongjiang Acheng province chemical reagent factory. HCl was provided from Shanghai Institute of Fine Chemical Technology. H_2O_2 was obtained from Tianli Chemical Reagent Co., Ltd. $NaNO_3$ was purchased from Tianjin Bodi Chemical Industry Co., Ltd. Urea was provided by Tianjin Zhiyuan Chemical Reagent Co., Ltd. Ferric chloride, $FeCl_3{\cdot}6H_2O$, was obtained from Tianli Chemical Reagent Co., Ltd. Glycine was obtained from Tianjin Guanfu Fine Chemical Research Institute and AP was purchased from Sinopharm Chemical Reagent Co., Ltd. All the reagents were of analytically pure grade (AR) and they were used without further purification.

2.2 *Preparation of α-Fe_2O_3 nanoparticles*

α-Fe_2O_3 nanoparticles were prepared by a facile hydrothermal method in the presence of ferric chloride hexahydrate ($FeCl_3{\cdot}6H_2O$) as the precursor. Initially, 3.47 g of $FeCl_3 \cdot 6H_2O$ was mixed with 100 ml of deionized water. The mixture was stirred until the $FeCl_3 \cdot 6H_2O$ was completely dissolved; later, 1.55 g of urea and 0.96 g of glycine were added to the mixture with stirring for 1 h. The mixture was sealed into a Teflon-lined stainless-steel autoclave and maintained at 180°C for 24 h, and then cooled to room temperature naturally. The resulting product was collected by centrifugation, washed several times with deionized water and ethanol and then dried at 60°C.

2.3 *Preparation of GO*

GO was synthesized from natural graphite by a modified Hummers method [15]. Graphite powder (1 g) and sodium nitrate (0.5 g) were mixed with 23 ml of concentrated sulphuric acid and stirred for 30 min in an ice bath; 3 g of potassium permanganate was then added gradually and stirred for 15 min. After that the mixture was transferred to a water bath and stirred for 30 min at 35°C. Next, 46 ml of deionized water was slowly added, and the temperature quickly rose from 35 to 98°C; the mixture was then maintained at this temperature for 30 min; 140 ml of deionized water and 5 ml of hydrogen peroxide were then added to the mixture and stirred for 2 h. At this stage the colour of the mixture changed from dark brown to brilliant yellow. Finally the mixture was separated by centrifugation, washed repeatedly with 5% HCl solution followed by deionized water until the mixture was neutral and then dried in vacuum.

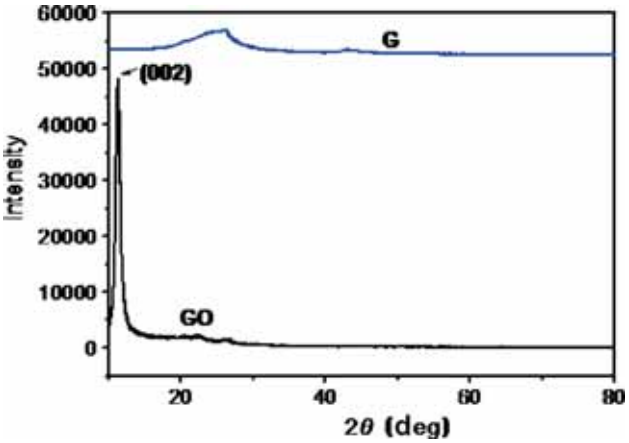

Figure 1. XRD patterns of GO and graphene.

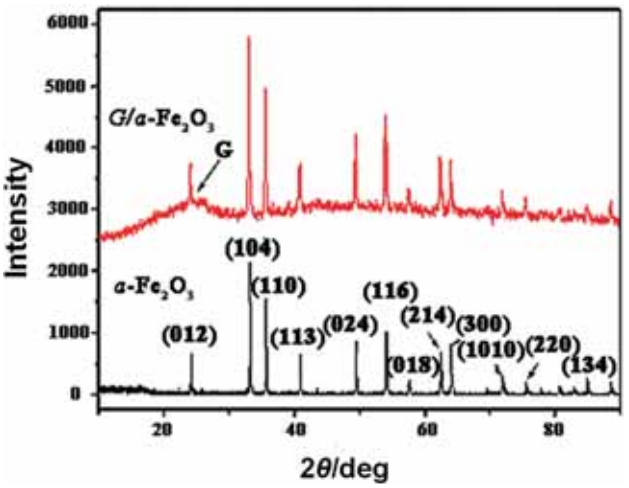

Figure 2. XRD patterns of **(a)** α-Fe_2O_3 and **(b)** G/α-Fe_2O_3 nanocomposites.

2.4 *Preparation of G/α-Fe_2O_3 nanocomposite*

G/α-Fe_2O_3 nanocomposite was prepared by *ex situ* synthesis, which is made by dispersing the as-prepared α-Fe_2O_3 nanoparticles directly into the GO solution; the percentage of GO and α-Fe_2O_3 in the composite was 75 and 25 wt%, respectively. The procedure was as follows: 0.12 g of GO was dissolved in 50 ml of deionized water and stirred overnight, 0.015 g of urea and 0.04 g of the as-prepared α-Fe_2O_3 were then added to the previous solution and stirred for 3 h; after this the mixture was transferred to a stainless-steel autoclave for the hydrothermal treatment at 120°C for 24 h. The nanocomposite was obtained after centrifugation, washed with deionized water and ethanol several times and then dried at 60°C. Graphene is obtained using the same method but in the absence of α-Fe_2O_3 nanoparticles.

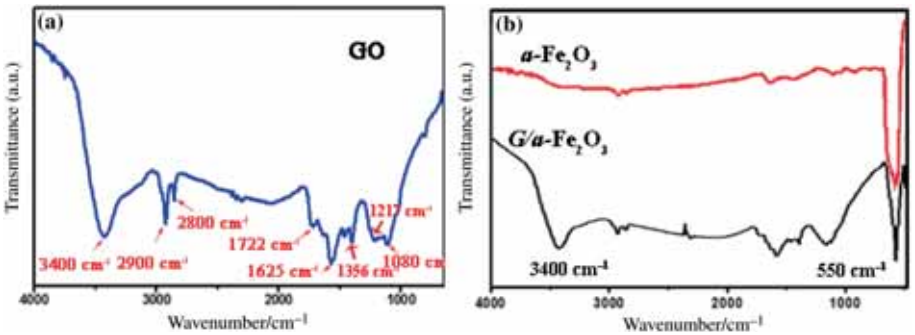

Figure 3. FTIR spectra of **(a)** GO, and **(b)** α-Fe_2O_3 and G/α-Fe_2O_3.

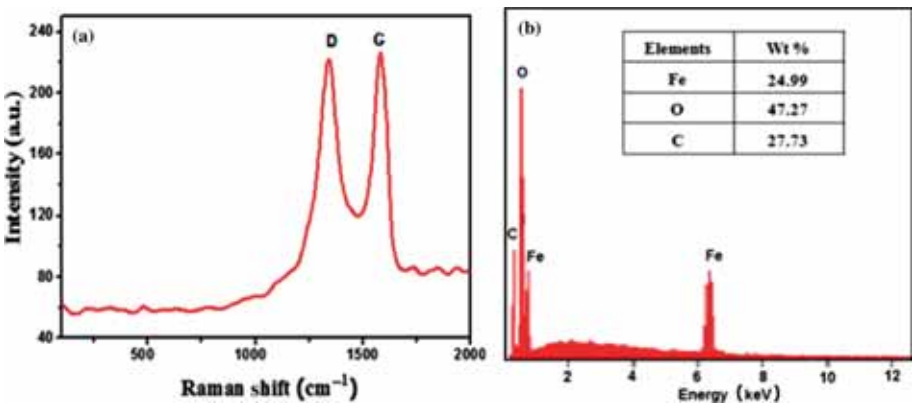

Figure 4. **(a)** Raman and **(b)** EDS spectra of G/α-Fe_2O_3.

2.5 *Materials characterization*

Powder X-ray diffraction (XRD) analyses of the samples were carried out with a (Rigaku TTR-III) equipped with Cu Kα radiation ($\lambda = 0.15406$ nm). The morphologies of the samples were investigated by scanning electron microscopy (SEM) using a JEOL Model JSM-6480 and transmission electron microscopy (TEM) using a JEM-2100 Model. The composition of the products was characterized by Fourier transform infrared spectroscopy (FT-IR spectra; Perkin Elmer Spectrum 100) in the range of 500−4000 cm^{-1}, the specific surface area (S_{BET}) of the nanomaterials was determined by nitrogen adsorption using Tri Star II 3020 surface Analyzer. The catalytic effect of the as-prepared additives on the thermal decomposition of AP was detected by TG–DTA at a heating rate of 10°C min^{-1} in a static N_2 atmosphere over the range of 50–500°C.

3. Results and discussion

3.1 *Characterization of samples*

Phase identification of the product was performed using powder XRD. Figure 1 shows the XRD patterns of the as-prepared GO and graphene; the characteristic (0 0 2) diffraction peak of GO appears at about 11°. After thermal reduction of GO, the XRD pattern of graphene shows a broad diffraction peak at about 25° and the disappearance of the diffraction peak at 11°. These results reveal that the GO is successfully reduced to graphene [16].

The XRD pattern of the as-prepared α-Fe_2O_3 (figure 2a) shows that the diffraction peaks of α-Fe_2O_3 appear at 24.2°, 33.2°, 35.6°, 40.9°, 49.5°, 54.1°, 57.6°, 62.4°, 64.0°, 71.9°, 75.4°, 85° and 88.5°, which correspond well with the crystal planes of (0 1 2), (1 0 4), (1 1 0), (1 1 3), (0 2 4), (1 1 6), (0 1 8), (2 1 4), (3 0 0), (1 0 10), (2 2 0), (1 3 4) and (2 2 6), respectively, for the hematite (JCPDS No. 33-0664). All the diffraction peaks are indexed as a rhombohedral crystalline phase (space group R-3c) of α-Fe_2O_3 with calculated lattice parameters $a = 5.036$ Å and $c = 13.749$ Å. No peaks of any other phases are detected from the XRD pattern, indicating that the as-prepared α-Fe_2O_3 particles are of high purity.

The XRD pattern of G/α-Fe_2O_3 nanocomposite (figure 2b) shows similar diffraction peaks as those of α-Fe_2O_3 nanoparticles; these diffraction peaks appear with good intensity compared with those of the pure α-Fe_2O_3. These results show that the hydrothermal treatment not only did not affect the crystalline phase of the hematite (α-Fe_2O_3) but also ameliorated its crystallinity. No apparent diffraction peaks of GO can

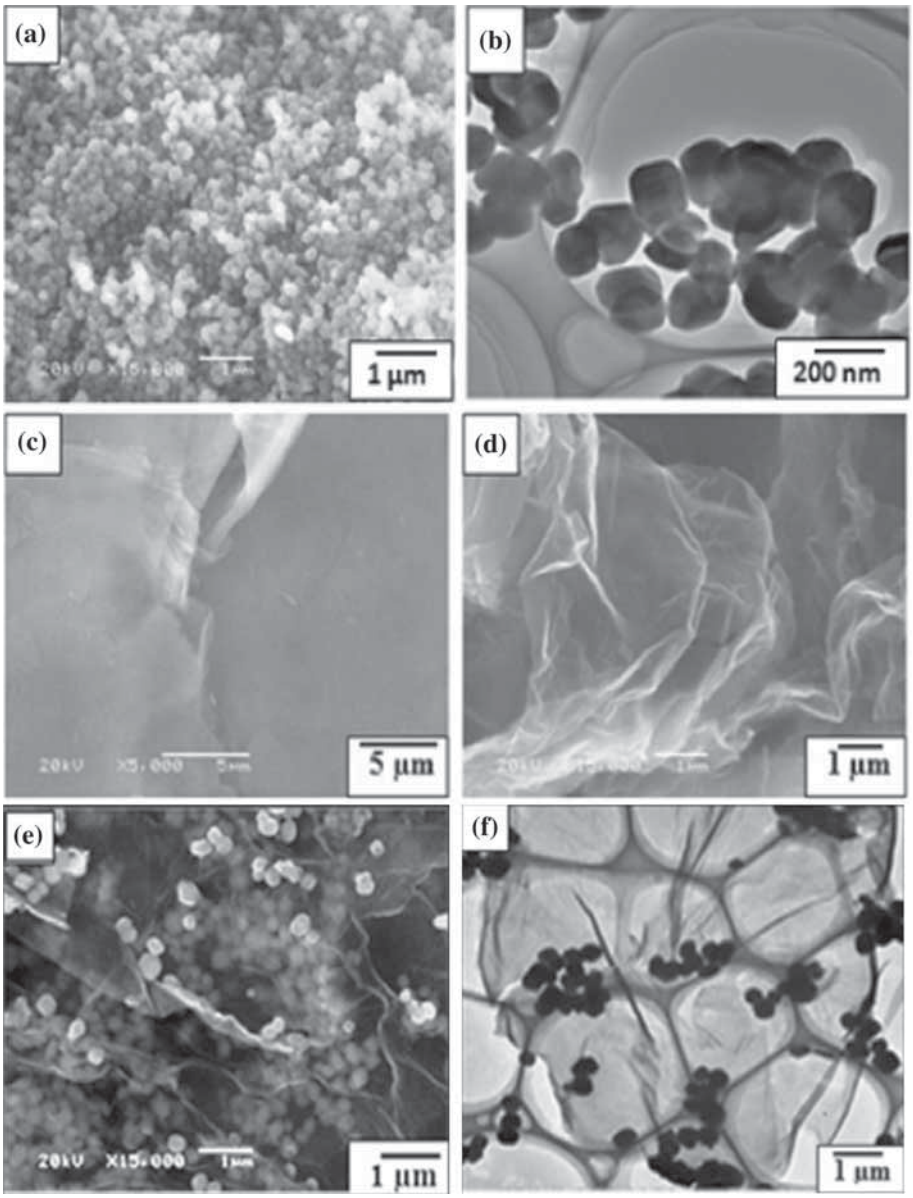

Figure 5. (**a**) SEM and (**b**) TEM images of a-Fe_2O_3, SEM images of (**c**) GO and (**d**) graphene, and (**e**) SEM and (**f**) TEM images of G/a-Fe_2O_3.

be detected in this XRD pattern; however, a broad diffraction peak of graphene was observed at about 26° and coincided with one of the diffraction peaks of α-Fe_2O_3, which shows that the GO was successfully reduced to graphene during the hydrothermal treatment.

In addition, to confirm the identification and the composition of the as-prepared materials, Fourier transform infrared spectroscopy (FTIR) investigations of GO, α-Fe_2O_3 and G/α-Fe_2O_3 give corresponding spectra as shown in figure 3a and b. The FTIR spectrum of pure GO (figure 3a) shows a strong and broad absorption at 3400 cm^{-1} due to the O–H stretching vibration of the adsorbed water molecules. The C=O stretching of COOH groups is observed at 1722 cm^{-1}. The stretching of the sp^2-hybridized C=C bond appears at 1625 cm^{-1}. The three peaks at 1356, 1217 and 1080 cm^{-1} are attributed to the stretching vibrations of carboxyl C=O, epoxy C–O and alkoxy C–O, respectively [17,18]. The absorption peak at 2800 and 2900 cm^{-1}represents the anti-symmetric stretching vibration of CH_2 and the stretching vibration of C–H, respectively [19].

The FTIR spectra of α-Fe_2O_3 and G/α-Fe_2O_3 nanocomposite show one similar absorption band at 550 cm^{-1} (figure 3b), which is due to the Fe–O vibrations [20]. A broad absorption band at 3400 cm^{-1} is also observed in the FTIR spectrum of G/α-Fe_2O_3 nanocomposite and it is attributed to the O–H stretching vibration of the adsorbed water [21].

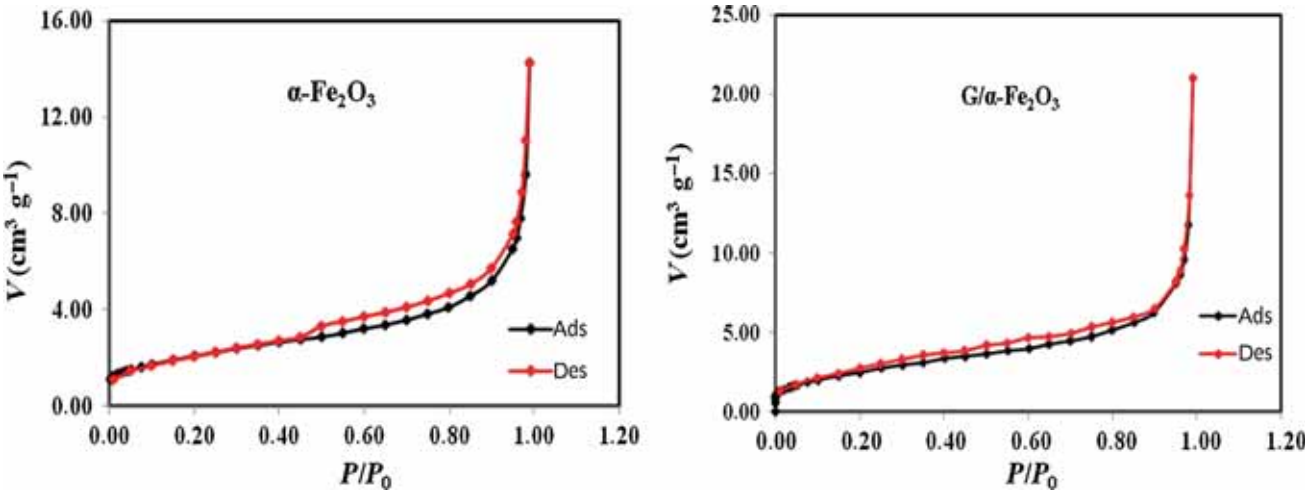

Figure 6. Adsorption and desorption isotherms for α-Fe_2O_3 and G/α-Fe_2O_3.

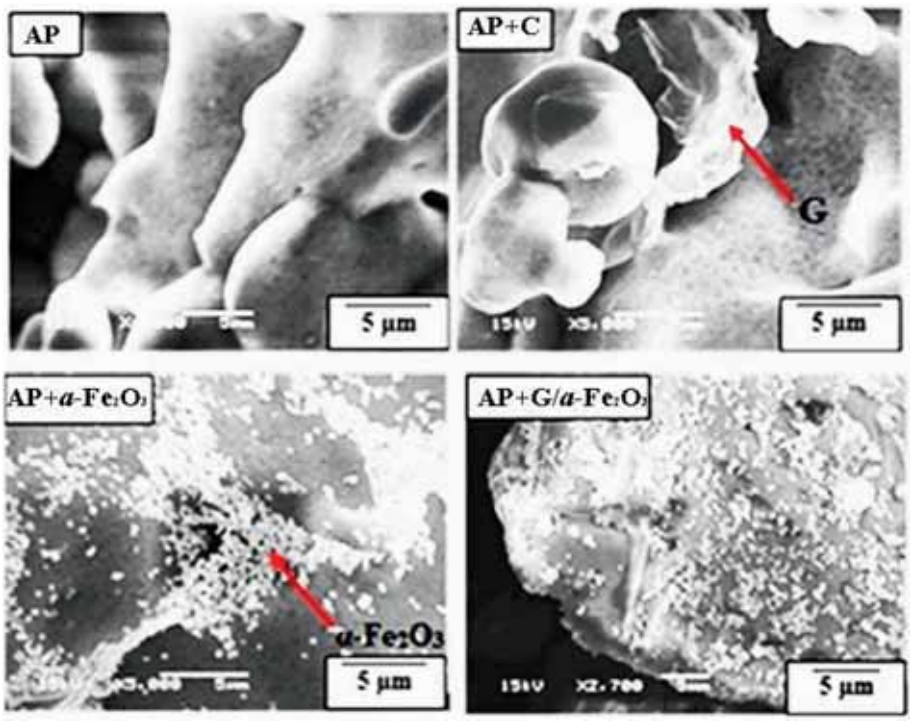

Figure 7. SEM images of AP, AP + G, AP + α-Fe_2O_3 and AP + G/α-Fe_2O_3.

The obtained G/Fe_2O_3 nanocomposite was also characterized by Raman spectroscopy and EDS. Figure 4a shows the Raman spectrum of this nanocomposite; two remarkable bands at 1343 and 1585 cm^{-1} are observed in this spectrum, which correspond to the D and the G band of graphene, respectively. The D band is attributed to the disorder and structural defects of graphene; however, the G band is related to the vibration of sp^2-bonded carbon [22]. Figure 4b shows the EDS spectrum of G/α-Fe_2O_3 nanocomposites and the percentages of its elements; the spectra show clearly the presence of three elements, which are iron (Fe), oxygen (O) and carbon (C).

The SEM and TEM images of the as-prepared α-Fe_2O_3 (figure 5a and b) reveal that the particles are spherical in shape with an average particle size of 150 nm. The SEM image of GO (figure 5c) shows smooth sheets with folded shapes; however, figure 5d depicts well-exfoliated graphene sheets, which have crumpled thin voile-like structures with folds. For the as-prepared G/α-Fe_2O_3 nanocomposite the SEM image (figure 5e) shows that α-Fe_2O_3 nanoparticles appear on both

sides of the graphene nanosheets; some of them are located above the graphene nanosheets, while others lie on the back of the nanosheets. However, the TEM images (figure 5f) show that α-Fe_2O_3 nanoparticles appear as small agglomerations on the graphene nanosheets.

The adsorption and desorption isotherms of nitrogen at −196°C obtained for α-Fe_2O_3 nanoparticles and G/α-Fe_2O_3 nanocomposite are presented in figure 6. The isotherms are identified as type IV. The BET surface area is found to be 7.543 $cm^2\ g^{-1}$ for α-Fe_2O_3 nanoparticles and 9.353 $cm^2\ g^{-1}$ for G/α-Fe_2O_3 nanocomposite.

3.2 *Thermal decomposition of AP in the presence of α-Fe_2O_3, graphene and G/α-Fe_2O_3 nanocomposite*

The catalytic effect of the as-prepared additives on the thermal decomposition of AP was detected by TG–DTA at a heating rate of 10°C min^{-1} in a static N_2 atmosphere over the range of 50–500°C. The SEM was also used to observe the morphology of the mixtures at room temperature. These mixtures were prepared as follows: 0.03 g of each additive was ground with 1.6 g of AP in the presence of ethanol solution in an agate mortar, and then dried in vacuum at room temperature. The SEM images of the pure AP and the three mixtures (AP + G, AP+α-Fe_2O_3 and AP+G/ α-Fe_2O_3) are shown in figure 7.

The SEM image of pure AP shows that it appears as connected clusters with a smooth surface; the presence of graphene nanosheets on the surface of AP is also observed for the mixture of AP + G; however, for the mixture of AP + α-Fe_2O_3 the SEM image shows different agglomerations of α-Fe_2O_3 nanoparticles on the surface of AP. In the case of AP + G/α-Fe_2O_3 these agglomerations disappear and well-distributed α-Fe_2O_3 nanoparticles are observed on the surface of AP.

The TG curve of pure AP (figure 8) shows that the mass loss starts at 320°C and is completed at 432°. However, the DTA curve reveals that the thermal decomposition of AP takes place in three stages.

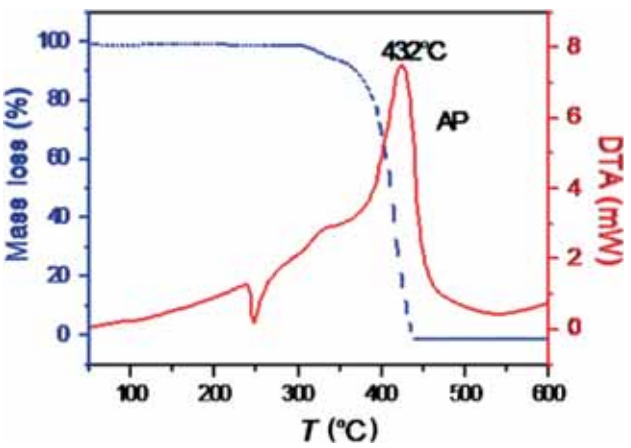

Figure 8. TG–DTA curves of pure AP.

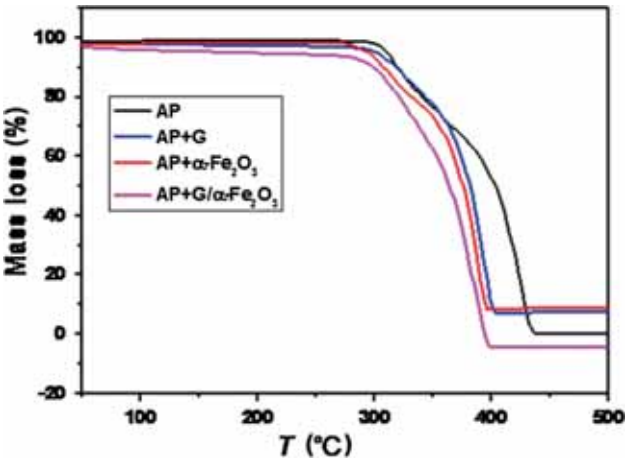

Figure 9. TG curves of AP, AP + G, AP + α-Fe_2O_3 and AP + G/α-Fe_2O_3.

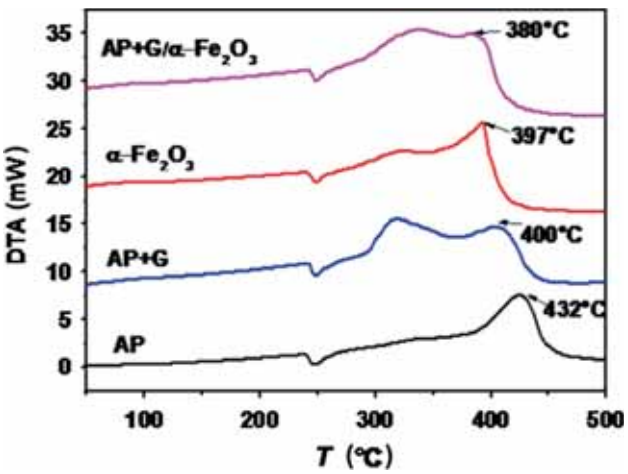

Figure 10. DTA curves of AP, AP + G, AP + α-Fe_2O_3 and AP + G/α-Fe_2O_3.

The first stage is the transition from orthorhombic to cubic form; this transition is characterized by an endothermic peak at 250°C. The second stage is due to the partial decomposition of AP where an exothermic peak appears at 320°C; it is also called as the low-temperature decomposition (LTD) step, which is a solid–gas multiphase reaction. The third stage is characterized by another exothermic peak at 432°C that indicates the complete decomposition of AP, which is also called as the high-temperature decomposition (HTD) step [23].

Figure 9 shows the TG curves of the mixtures of AP with the as-prepared nanoadditives. For all the curves the mass loss starts at T around 320°C. However, it finishes at different temperatures and they are all lower than that of pure AP (432°C).

The DTA curves of the mixtures of AP with the nanoadditives (figure 10) show that for all the mixtures there is no change in the transition phase of AP. However, the only change appears in the HTD step. Considering that the thermal decomposition of AP follows the electron transfer process

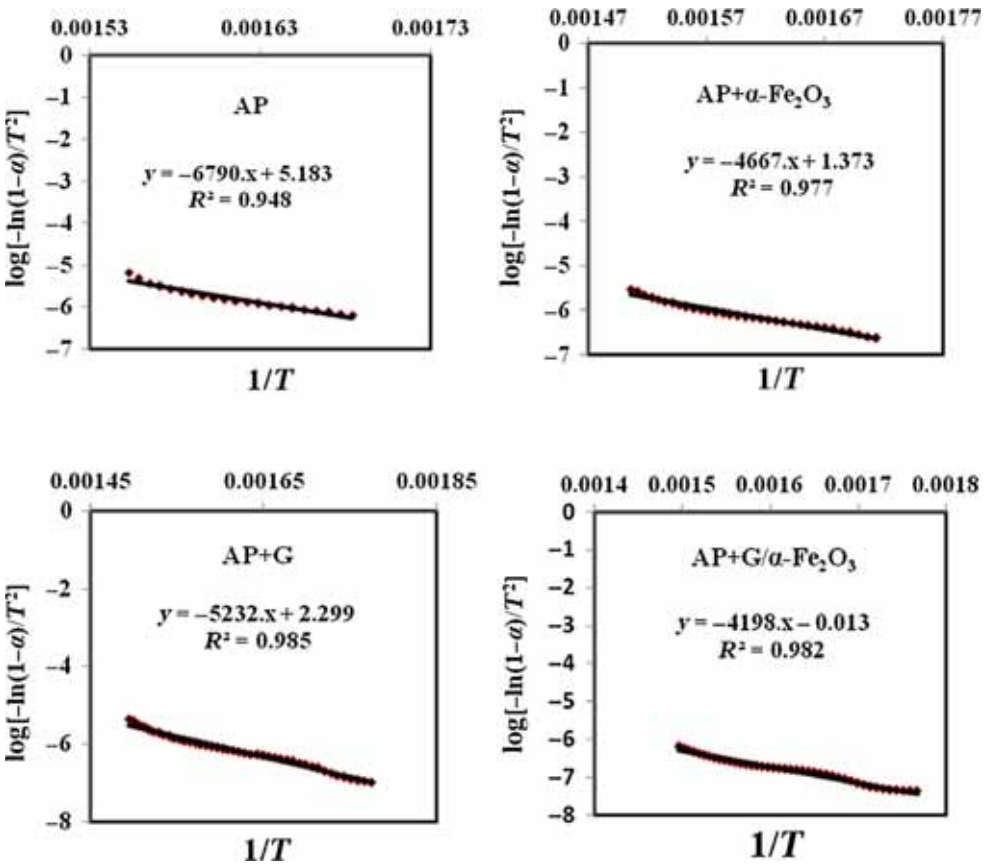

Figure 11. Coats–Redfern plot of AP, AP + G, AP + α-Fe_2O_3 and AP + G/α-Fe_2O_3.

[24], the reaction takes place when electrons are transferred from anions to cations.

A diminution of the high temperature of decomposition of AP by 32°C was achieved in the presence of graphene (figure 10), due to its high electron mobility. However, in the presence of α-Fe_2O_3 nanoparticles the HTD of AP decreases from 430 to 397°C. In the case of the mixture of AP + G/α-Fe_2O_3, the results of DTA show that G/α-Fe_2O_3 nanocomposite gives even better results with a reduction in the HTD of AP from 430 to 380°C.

Table 1. Activation energy (E_a), high-temperature decomposition peak (HTD) and correlation coefficient (r) for the decomposition of AP with the as-prepared nanoadditives.

Composition	HTD (°C)	E_a (kJ mol^{-1})	r
AP	432	129	0.94
AP + α-Fe_2O_3	397	89.31	0.97
AP + G	400	100.12	0.98
AP + G/α-Fe_2O_3	380	80.33	0.98

3.3 *Kinetics studies*

The activation energy of the thermal decomposition of AP with the as-prepared nanoadditives is determined using the method of Coats–Redfern based on the following equation for $n = 1$ [25]:

$$\log\left[\frac{-\ln(1-\alpha)}{T^2}\right] = \log\frac{AR}{\beta E} - \frac{E}{2.303RT},$$

where α is the extent of conversion, T is the temperature, A is the pre-exponential factor, R the universal gas constant, E the activation energy and β the heating rate. The value of the activation energy will be obtained from the slope of the straight line obtained by the graphic representation of $\log[-\ln(1-\alpha)/T^2]$ *vs.* $[1/T]$ as shown in figure 11.

Table 1 presents the values of the HTD peaks, the correlation coefficient and the activation energy of pure AP and the three mixtures of AP with additives. The table shows that each decrease in the peak value of HTD corresponds also to a decrease in the value of the activation energy and the lowest one (80.33 kJ mol^{-1}) is attributed to the mixture of AP+G/α-Fe_2O_3.

Although graphene has high electron mobility, its catalytic activity is much lower than that of α-Fe_2O_3 nanoparticles. These results show that the catalytic activity of additives does not depend only on their electron mobility but it is also

related to their electron configuration. Due to their small size, α-Fe_2O_3 nanoparticles present a lot of active sites on their surface; these active sites are the place where the catalytic process takes place. The catalytic process of α-Fe_2O_3 nanoparticles is a process of complex formation between the metal cation Fe^{3+} and the perchlorate anion; these cations are electrically unsaturated and tend to attract electrons from the oxygen atoms in the perchlorate anion; this interaction can weaken the oxygen–chlorine bond in the perchlorate anion and therefore accelerate its thermal decomposition. The presence of the two additives together in the form of G/α-Fe_2O_3 nanocomposite gives better result than that of α-Fe_2O_3 nanoparticles due to the presence of graphene, which plays two roles: first by its high electron mobility and second by decreasing the agglomeration of α-Fe_2O_3 nanoparticles and therefore increasing the number of active sites in the nanocomposite.

4. Conclusions

α-Fe_2O_3, graphene and G/α-Fe_2O_3 nanocomposite are successfully obtained by a simple hydrothermal method and show an intensive catalytic effect on the thermal decomposition of AP. The results of DTA indicate that the presence of the two additives together in the form of G/α-Fe_2O_3 nanocomposite gives an improved performance accompanied by a diminution of HTD peak value and the activation energy by 50°C and 48.67 kJ mol^{-1}, respectively.

Acknowledgements

This work was supported by Heilongjiang Province Natural Science Funds for Distinguished Young Scholar, Special Innovation Talents of Harbin Science and Technology for Distinguished Young Scholar (2014RFYXJ005), Fundamental Research Funds of the Central University (HEUCFZ, HEUCFD1404), Natural Science Foundation of Heilongjiang Province (B201316), Program of International S&T Cooperation Special Project (2013DFR50060), Special Innovation Talents of Harbin Science and Technology (2014RFQXJ087) and the fund for Transformation of Scientific and Technological Achievements of Harbin (2013DB4BG011).

References

[1] Satyawati S, Patil P R and Krishnamurthy V N 2008 *Defence Sci. J.* **58** 721
[2] Zhu Y, Murali S and Cai W 2010 *Adv. Mater.* **22** 3906
[3] Stankovich S, Dikin D A and Piner R D 2007 *Carbon* **45** 1558
[4] Xu Y, Sheng K and Li C 2010 *ACS Nano* **4** 4324
[5] Ajaz A G 1995 *J. Hazard. Mater.* **42** 303
[6] Shusser M, Culick F E C and Cohen N S 2002 *J. Propul. Power* **18** 1093
[7] Survase D, Gupta M and Asthana S 2002 *Prog. Cryst. Growth Charact. Mater.* **32** 161
[8] Rocco J, Lima J, Frutuoso A *et al* 2004 *J. Therm. Anal. Calorim.* **75** 551
[9] Chaturvedi S and Dave P N 2013 *J. Saudi Chem. Soc.* **17** 135
[10] Liu L, Li F and Tan L 2004 *Propell. Explos. Pyrotech.* **29** 34
[11] Chen L, Li L and Li G 2008 *J. Alloys Compd.* **464** 532
[12] Singh S, Srivastava P, Kapoor I *et al* 2013 *J. Therm. Anal. Calorim.* **111** 1073
[13] Yu Z, Sun Y, Wei W *et al* 2009 *J. Therm. Anal. Calorim.* **97** 903
[14] Wang Y, Zhu J, Yang X *et al* 2005 *Thermochim. Acta* **437** 3
[15] Hummers W S and Offeman R E 1958 *J. Am. Chem. Soc.* **80** 1339
[16] Hu H, Liu Y and Wang Q 2011 *Mater. Lett.* **65** 2582
[17] Wojtoniszak M, Chen X and Kalenczuk R J 2012 *J. Colloids Surf.* **89** 79
[18] Guo S, Zhang G and Guo Y 2013 *Carbon* **60** 437
[19] Shahriary L and Athawale A 2014 *Int. J. Renew. Energy Environ. Eng.* **02** 58
[20] Yariv S and Mendelovici E 1979 *Appl. Spectrosc.* **33** 410
[21] Reid D L, Russo A E and Carro R V 2007 *Nano Lett.* **7** 2157
[22] Yang D, Velamakanni A, Bozoklu G, Park S, Stoller M, Piner R *et al* 2009 *Carbon* **47** 145
[23] Reid D L, Russo A E, Carro R V, Stephens M A, Spalding T C, Petersen E L *et al* 2007 *Nano Lett.* **7** 2157
[24] Boldyrev V V 2006 *Thermochim. Acta* **443** 1
[25] Coats A W and Redfern J P 1964 *Nature* **201** 68